RIEMANNIAN SPARSE CODING FOR CLASSIFICATION OF POLSAR IMAGES

Wen Yang[1], *Neng Zhong*[1], *Xiangli Yang*[1], *Anoop Cherian*[2]

[1]School of Electronic Information, Wuhan University, 430072 Wuhan, China
[2]Australian Centre for Robotic Vision, Australian National University, Acton, ACT 2601, Australia

ABSTRACT

Hermitian positive definite (HPD) covariance matrices form one of the most widely-used data representations in PolSAR applications. However, most of these applications either use statistical distribution models on the PolSAR covariance matrices or polarimetric target decomposition. In this paper, we study HPD matrices for PolSAR image classification in the context of sparse coding. More specifically, the PolSAR HPD matrices are first represented as sparse linear combinations of elements from a dictionary, where each element itself is an HPD matrix and the representation loss is measured by the affine-invariant Riemannian metric. We then introduce a sparsity induced similarity measure between two HPD matrices. Finally, we propose a supervised classification scheme using support vector machines on the Riemannian sparse codes and an unsupervised classification scheme encompassing a sparsity induced similarity measure followed by spectral clustering. The proposed methods are validated on the NASA/JPL AIRSAR fully PolSAR data. The experimental results demonstrate the effectiveness of our methods.

Index Terms— PolSAR, Riemannian sparse coding, clustering, classification.

1. INTRODUCTION

Fully Polarimetric Synthetic Aperture Radar (PolSAR) is a technology for long-term monitoring of the Earth's surface based on multi-dimensional measurements via transmitting microwave pulses with two distinct orthogonal polarizations. As a crucial step for the automatic interpretation of PolSAR data, image classification plays a significant role in many important applications, including land-cover mapping and damage assessment for environmental disasters.

The covariance matrices - which are one of the classical descriptors on PolSAR data – have been used in many classification applications. To make full use of the information contained in PolSAR covariance matrices, many schemes have been proposed in the past years. Based on the logarithmic likelihood function of complex Wishart distribution model, Lee et al. [1] introduced the Wishart distance and proposed a maximum likelihood classifier on PolSAR images. By taking advantage of statistical hypothesis test theory, Kersten et al. [2] proposed Bartlett distance to measure the similarity of two sample covariance matrices and Song et al. [3] applied it in unsupervised classification for large scale PolSAR images. Considering that covariance matrices are Hermitian positive definite and form a differentiable Riemannian manifold, geodesic distance on the manifold is a more suitable measure to describe the similarity between two covariance matrices. Two popular geodesic distances on the Riemannian manifold of HPD matrices are the affine-invariant Riemannian metric (AIRM) [4] and log-Euclidean Riemannian metric (LERM) [5]. Due to the computational complexity, LERM is more practical compared to AIRM. To further reduce the computational cost, Cherian et al. [6] introduced Jensen-Bregman LogDet divergence (JBLD), which is not a Riemannian metric, however has close connections to AIRM and is generally seen to perform similar. Chen et al. [7] reviewed notable advances of polarimetric target decomposition and discusses further developments. However, most of these methods use the statistical distribution models of the PolSAR covariance matrices or polarimetric target decompositions.

In this paper, we study HPD matrices for PolSAR image classification based on Riemannian sparse coding (RSC). The remainder of this paper is organized as follows. Section 2 presents the Riemannian sparse coding for HPD matrices, and then introduces a sparse induce similarity measure between two covariance matrices. In Section 3, the experimental results of proposed methods for both supervised and unsupervised classification are reported. Section 4 draws the conclusions.

2. PRELIMINARIES

2.1. PolSAR Covariance Matrices

In general, the polarimetric information of the backscatter microwave within every resolution cell can be represented by a complex vector $\mathbf{u} = [S_{hh}\ \sqrt{2}S_{hv}\ S_{vv}]^T$, where the superscript ^{T} denotes the matrix transpose. To reduce the speckle noise, SAR data are usually multi-look processed. The multi-look PolSAR data can be represented by the polarimetric co-

The research was partially supported by the National Key Basic Research and Development Program of China under Contract 2013CB733404 and the Chinese National Natural Sciences Foundation grants (No.61271401, No.61331016).

variance matrix:

$$\mathbf{C} = \frac{1}{n}\sum_{i=1}^{n}\mathbf{u}_i\mathbf{u}_i^H, \tag{1}$$

where superscript ^{H} denotes the Hermitian transpose, and n is the number of looks. These polarimetric covariance matrices are Hermitian positive definite matrices, which forms a Riemannian manifold instead of a Euclidean space [8].

2.2. Riemannian Sparse Coding for HPD Matrices

Inspired by the great success of sparse coding for vector valued data, Cherian et al. [9] proposed the Riemannian sparse coding scheme for symmetric positive definite (SPD) matrices, which measures sparse reconstruction loss using the affine-invariant Riemannian metric. Here we extend this setup into HPD matrices for processing PolSAR images. The HPD matrices are expressed as sparse linear combinations of elements from a dictionary, where each element itself is an HPD matrix.

Given a dictionary B which is formed by HPD matrices $\{\mathbf{B}_1, \mathbf{B}_2, \ldots, \mathbf{B}_k\} \in \mathbf{S}_{++}^n$, the HPD matrix $\mathbf{X}$ can be sparse coded by the dictionary B. The aim of Riemannian sparse coding for HPD matrices is to obtain a nonnegative sparse vector $\boldsymbol{\alpha} = [\alpha_1, \alpha_2, \ldots, \alpha_k]^T$, which makes the linear combination $\sum_{i=1}^{k}\alpha_i\mathbf{B}_i$ approximate to matrix $\mathbf{X}$ under the geodesic distance for AIRM. Thus, we can write the sparse coding problem as follows:

$$\min_{\boldsymbol{\alpha}\succeq 0}\ \phi(\boldsymbol{\alpha}) := \frac{1}{2}d^2(\mathbf{X}, \sum_{i=1}^{k}\alpha_i\mathbf{B}_i) + \mathrm{S}(\boldsymbol{\alpha}). \tag{2}$$

The affine-invariant Riemannian metric (AIRM) [4], as one of the most popular intrinsic metric on the HPD manifold, is defined as $d(\mathbf{X}, \mathbf{Y}) = \|\log(\mathbf{X}^{-\frac{1}{2}}\mathbf{Y}\mathbf{X}^{-\frac{1}{2}})\|_{\mathrm{F}}$, where log is the principal matrix logarithm. It has been proved in [9] that $\phi(\alpha) := \frac{1}{2}d^2(\mathbf{X}, \sum_{i=1}^{k}\alpha_i\mathbf{B}_i)$ is a convex function on the set

$$\mathrm{C} := \{\boldsymbol{\alpha} | \sum_{i=1}^{k}\alpha_i\mathbf{B}_i \preceq \mathbf{X}, \text{ and } \alpha_i \geq 0\}, \tag{3}$$

then the sparse coding problem for HPD matrices can be rewritten as equation (4), where $\lambda \geq 0$ is a regularization parameter.

$$\min_{\boldsymbol{\alpha}\succeq 0}\phi(\boldsymbol{\alpha}) := \frac{1}{2}\|\log(\sum_{i=1}^{k}\alpha_i\mathbf{X}^{-\frac{1}{2}}\mathbf{B}_i\mathbf{X}^{-\frac{1}{2}})\|_{\mathrm{F}}^2 + \lambda\|\boldsymbol{\alpha}\|_1. \tag{4}$$

With the constraints in (3), the problem (4) is a regularized nonnegative convex optimization problem which can be solved by the spectral projected gradient algorithm [10].

2.3. Sparsity Induced Similarity for HPD Matrices

Inspired by the sparsity induced similarity (SIS) measure for the vector values [11], we introduce the sparsity induced similarity measure for PolSAR HPD matrices.

Let $\mathrm{F} = \{\mathbf{F}_1, \mathbf{F}_2, \ldots, \mathbf{F}_N\} \in \mathbf{S}_{++}^n$ denotes the set of HPD matrices, the Riemannian sparse coding dictionary B_k of matrix $\mathbf{F}_k$ is formed by the remaining set $\{\mathbf{F}_1, \ldots, \mathbf{F}_{k-1}, \mathbf{F}_{k+1}, \ldots, \mathbf{F}_N\}$ denotes the dictionary of HPD matrix $\mathbf{F}_k$, then the vector $\boldsymbol{\alpha}_k = [\alpha_1, \ldots, \alpha_{k-1}, \alpha_{k+1}, \ldots, \alpha_N]^T$ can be obtained by Riemannian sparse coding. The sparsity induced similarity between matrices $\mathbf{F}_i (1 \leq i \leq N, i \neq k)$ and $\mathbf{F}_k$ is defined as $s_{ki} = \alpha_i / \sum_{j=1, j\neq k}^{N}\alpha_j$. After repeating this step for every matrix, a similarity matrix $\mathbf{S}$ is obtained. Considering the symmetry of similarity matrix, the final similarity matrix $\mathbf{W}$ can be defined as

$$\mathbf{W}_{ij} = \begin{cases} \dfrac{s_{ij} + s_{ji}}{2} & (i \neq j) \\ 1 & (i = j) \end{cases}. \tag{5}$$

3. PROPOSED METHODS AND EXPERIMENT

3.1. Supervised Classification

The processing workflow of the proposed supervised classification can be itemized into three steps. First, the dictionary is obtained by clustering HPD matrices of PolSAR data or directly learning a dictionary via a Riemannian geometric approach [10]. Then, every HPD matrix is represented as sparse linear combination of elements from the dictionary by Riemannian sparse coding. Next, the sparse code vector $\boldsymbol{\alpha}$ for each matrix is used to train a support vector machine (SVM) for classification.

To investigate the effectiveness of the proposed supervised classification method, we use an AIRSAR L-band fully PolSAR image. The image was acquired over from Flevoland, Netherlands in 1989 and its size is 750×1024 pixels. Fig. 1(a) and (b) show its RGB composite image and ground truth map, respectively. Fig. 1(f) defines eleven classes with their color codes, i.e., bean, forest, potato, alfalfa, wheat, bare land, beet, rape, pea, grass and water.

We use 500 points, randomly sampled from defined areas, for every class to form the training set and the rest as the test set. The classical maximum likelihood (ML) classifier based on Wishart distance (denoted by Wishart-ML) and JBLD (denoted by JBLD-ML) are respectively employed to make a comparison with the proposed method (denoted by RSC-SVM). As suggested in [9], the dimension of dictionary is fixed at 30, and the dictionary is obtained by the K-means clustering algorithm with log-Euclidean Riemannian metric. The regularization parameter λ in the Riemannian sparse coding is set to 100. The parameters of LIBSVM for radial basis function are selected via cross-validation. The overall accuracy (OA) (higher is better) and Kappa coefficient (higher is better) [12] are used to evaluate the performance of different supervised classification methods. The experimental results of different classification methods are shown in Fig. 1(c) $\sim$ (e) and performance evaluation is shown in Table 1.

As expected, results obtained without considering spatial dependencies are rather noisy due to speckle noise. Howev-

er, the main land cover types are well distinguished by the proposed method. It can be seen in Fig. 1(c) and 1(d) that classification results of Wishart-ML and JBLD-ML are poor, especially those classes of wheat, grass and alfalfa. While in Fig. 1(e), wheat, grass and alfalfa area are correctly classified. Furthermore, the noises in the same classified area are less in Fig. 1(e) than Fig. 1(c) or 1(d). We can observe that our method obtains the highest values of OA and kappa among the three different classification methods. That is to say our method achieved superior classification performance.

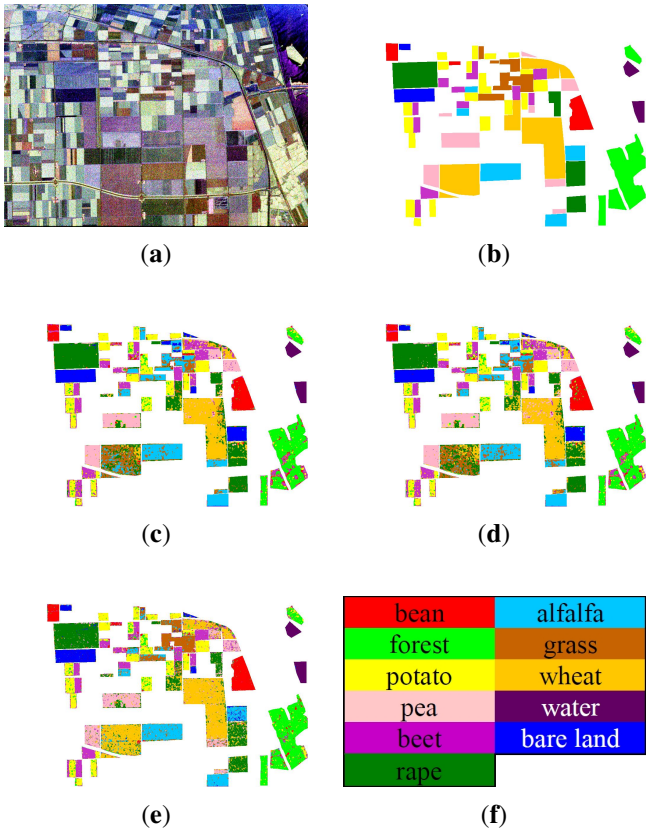

Fig. 1. AIRSAR L-band PolSAR image of Flevoland in 1989. (**a**) Pauli RGB for the original image. (**b**) Ground truth map. (**c**) Wishart-ML result. (**d**) JBLD-ML result. (**e**) RSC-SVM result. (**f**) Color code.

Table 1. The OA and Kappa value of different supervised classification methods.

Method	OA	Kappa
Wishart-ML	0.6862	0.6476
JBLD-ML	0.6922	0.6534
RSC-SVM	0.8230	0.7984

3.2. Unsupervised Classification

The processing workflow for unsupervised classification contains three steps: (i) generating superpixels, (ii) computing SIS matrix, and (iii) spectral clustering. Before computing the SIS matrix, a simple linear iterative clustering algorithm, adapted for PolSAR image [3], is employed to generate a superpixels. It not only reduces the number of HPD matrices, but also implicitly introduces spatial constraints. Given a superpixel F_k, we choose the first m superpixels which are closest to F_k in terms of JBLD distance (instead of all the remaining superpixels) to form the dictionary B_k. The value of m should be carefully considered to get the better classification results. With the SIS matrix obtained, spectral clustering algorithm is employed to get the final unsupervised classification results.

To assess the performance of the proposed method, we use an AIRSAR L-band fully PolSAR image with size of 430×280 pixels. The image is obtained from the Flevoland test site in 1991. The RGB composite image is shown in Fig. 2(a). The ground truth map is shown in Fig. 2(b), in which seven classes are defined. Fig. 2(g) defines their color codes, i.e., beet, flax, grass, potato, wheat, rape, and barley. The classical iterative Wishart classifier [1] (denoted by Wishart-K) is used as the baseline. A K-means algorithm with JBLD (denoted by JBLD-K) is also investigated. We implemented a large scale spectral clustering algorithm with spatial constraints [3] (denoted by LSC) for comparing to the proposed unsupervised classification method (denoted by RSC-SIS).

For LSC and RSC-SIS, we chose $N_s = 5, N_m = 0.1$ in the SLIC algorithm to generate superpixels. The dictionary size of B_k and regularization parameter λ are set as 500 and 10 respectively in Riemannian sparse coding. To assess the strength of different unsupervised classification methods, evaluation metrics based on purity and entropy [13] are adopted. A higher value of purity and a lower value of entropy indicate a better performance of unsupervised classification solution. Taking into account the undefined land areas (void), the whole image is clustered into eight classes in the experiments. However, we ignore the void pixels during evaluation. The experimental results of different classification methods are shown in Fig. 2(c) $\sim$ (f) and performance evaluation is shown in Table 2.

Fig. 2(c) and 2(d) show the classification results of Wishart-K and JBLD-K methods respectively, with noise in the homogeneous regions that lacks spatial information. The classification results for LSC and RSC-SIS are shown in Figure 2(e) and 2(f), and it can be seen that different land classes are well distinguished and homogeneous areas are much smoother with the introduction of spatial constraints. The proposed method obtains the highest value of purity and the lowest value of entropy. As expected, the quantitative analysis demonstrates the superior performance of our method.

4. CONCLUSIONS

In this paper, we have presented PolSAR image classification methods using Riemannian sparse coding for HPD matri-

ces. The qualitative and quantitative analysis of experimental results demonstrate the superior performance of our methods in classification accuracy and clustering quality compared to the competitors. In future, we will extend the proposed method to other PolSAR applications, such as object recognition and change detection.

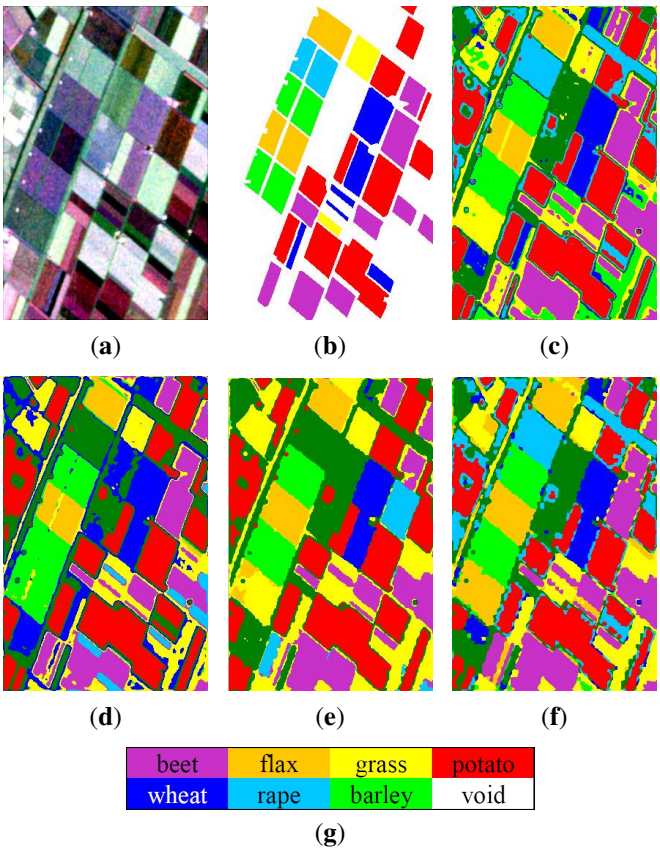

Fig. 2. AIRSAR L-band PolSAR image of Flevoland in 1991. (**a**) Pauli RGB for the original image. (**b**) Ground truth map. (**c**) Wishart-K result. (**d**) JBLD-K result. (**e**) LSC result. (**f**) RSC-SIS result. (**g**) Color code.

Table 2. The Purity and Entropy values of different unsupervised classification methods.

Method	Purity	Entropy
Wishart-K	0.9157	0.1190
JBLD-K	0.9259	0.1162
LSC	0.9259	0.0892
RSC-SIS	0.9311	0.0856

5. REFERENCES

[1] J. S. Lee, M. R. Grunes, and R. Kwok, "Classification of multi-look polarimetric SAR imagery based on complex Wishart distribution," *Int. J. Remote Sens.*, vol. 15, no. 15, pp. 2299–2311, 1994.

[2] P. R. Kersten, J. S. Lee, and T. L. Ainsworth, "Unsupervised classification of polarimetric synthetic aperture radar images using fuzzy clustering and EM clustering," *IEEE Trans. Geosci. Remote Sens.*, vol. 43, no. 3, pp. 519–527, 2005.

[3] H. Song, W. Yang, Y. Bai, and X. Xu, "Unsupervised classification of polarimetric SAR imagery using large-scale spectral clustering with spatial constraints," *Int. J. Remote Sens.*, vol. 36, no. 11, pp. 2816–2830, 2015.

[4] X. Pennec, P. Fillard, and N. Ayache, "A riemannian framework for tensor computing," *Int. J. Comput. Vision*, vol. 66, no. 1, pp. 41–66, 2006.

[5] V. Arsigny, P. Fillard, X. Pennec, and N. Ayache, "Log-euclidean metrics for fast and simple calculus on diffusion tensors," *Magn. Reson. Med.*, vol. 56, no. 2, pp. 411–421, 2006.

[6] A. Cherian, S. Sra, A. Banerjee, and N. Papanikolopoulos, "Jensen-bregman logdet divergence with application to efficient similarity search for covariance matrices," *IEEE Trans. Pattern Anal. Mach. Intell.*, vol. 35, no. 9, pp. 2161–2174, 2013.

[7] S. Chen, Y. Li, X. Wang, and S. Xiao, "Modeling and interpretation of scattering mechanisms in polarimetric synthetic aperture radar: Advances and perspectives," *IEEE Signal Process. Mag.*, vol. 31, no. 4, pp. 79–89, 2014.

[8] W. Yang, H. Song, G.-S. Xia, and C. López-Martínez, "Dissimilarity measurements for processing and analyzing polsar data: A survey," in *IGARSS*, 2015.

[9] A. Cherian and S. Sra, "Riemannian sparse coding for positive definite matrices," in *ECCV*, 2014.

[10] A. Cherian and S. Sra, "Riemannian dictionary learning and sparse coding for positive definite matrices," *arXiv:1507.02772[cs.CV]*, 2015.

[11] H. Cheng, Z. Liu, L. Hou, and J. Yang, "Sparsity induced similarity measure and its applications," *IEEE Trans. Circ. Syst. Video. Tech.*, vol. 26, no. 4, pp. 613–626, 2012.

[12] G. M. Foody, "Status of land cover classification accuracy assessment," *Remote Sens. Environ.*, vol. 80, no. 1, pp. 185–201, 2002.

[13] K. Xu, W. Yang, G. Liu, and H. Sun, "Unsupervised satellite image classification using markov field topic model," *IEEE Geosci. Remote Sens. Lett.*, vol. 10, no. 1, pp. 130–134, 2013.